No. 12, 1984, pp. 1827, 1828.
[9]Kabe, A. M., "Stiffness Matrix Adjustment Using Mode Data," *AIAA Journal,* Vol. 23, No. 9, 1985, pp. 1431–1436.
[10]Caesar, B., "Update and Identification of Dynamic Mathematical Models," *Proceedings of the 4th International Modal Analysis Conference,* Society for Experimental Mechanics and Union College, Los Angeles, CA, Feb. 1986, pp. 394–401.
[11]Kammer, D. C., "Optimum Approximation for Residual Stiffness in Linear System Identification," *AIAA Journal,* Vol. 26, No. 1, 1988, pp. 104–112.
[12]Zhang, D.-W., and Li, J.-J., "A New Method for Updating the Dynamic Mathematical Model of a Structure," Inst. of Aeroelasticity, DFVLR IB 232-87 J05, Gottingen, Germany, Dec. 1987.
[13]Wei, F. S., and Zhang, D.-W., "Mass Matrix Modification Using Element Correction Method," *AIAA Journal,* Vol. 27, No. 1, 1989, pp. 119–121.

Study of the Coupled Free Vibration of Helical Springs

W. Jiang,* T. L. Wang,† and W. K. Jones‡
Florida International University, Miami, Florida 33199

Introduction

THE study of helical spring dynamics can be dated back as early as 1890, when Michell[1] obtained three equations of motion by using the first form of Lagrange's fundamental equation. In the derivation, Michell considered displacements in three directions, but only one independent rotation. All of the moments of inertia of the typical element and the deformation produced by all forces were ignored. He showed the existence of two types of wave, producing axial or radial movement. These two waves were independent.

Love[2] obtained six equations of motion based on the same assumptions as Michell's. His equations were later modified by Yoshimura and Murata[3] to include the torsional inertia, and then by Wittrick[4] to include the rotary inertia and Timoshenko shear-deformation effects. The governing equations thus derived, however, are too difficult to permit analytical solutions. Consequently, various numerical methods, together with a variety of simplifications, were introduced to attack such problems (e.g., Mottershead,[5] Pearson and Wittrick[6]). Interested readers can refer to an extensive literature review by Pearson.[7]

Some "simple" theories were also developed along with the aforementioned "complex" theories. The simplest one treated the spring as a homogeneous rod having modified elastic and mass properties (e.g., Dick,[8] Gross,[9] Curran[10]). The coupling effects relating extension, torsion, and bending were ignored. Phillips and Costello[11] extended the simple theory to include the extensional-torsional coupling effect for springs under the action of axial forces and moments, and a set of nonlinear equations was obtained. Costello[12] further extended the investigation in the radical expansion due to axial impact, and the linear and nonlinear theories were compared in a paper by Sinha and Costello.[13]

Based on the simple theory, closed-form solutions to the coupled free vibration of helical springs have been achieved in a previous paper.[14] This Note uses examples to further explore the characteristics of the coupled vibration.

Received Dec. 3, 1990; revision received July 1, 1991; accepted for publication Aug. 4, 1991. Published by the American Institute of Aeronautics and Astronautics, Inc., with permission.

*Assistant Professor, Mechanical Engineering Department.
†Associate Professor, Civil Engineering Department.
‡Associate Professor, Mechanical Engineering Department.

Free Vibration of Helical Springs

It has been shown in the previous research that the static and dynamic responses of helical springs are coupled, that is, a tensile load will cause both axial and rotational displacements at the same time, and conversely, a torque will result in rotation as well as extension. Let u and θ be the axial and rotational displacement. Then the equations of motion of the spring can be expressed as

$$k_1 \frac{\partial^2 u}{\partial x^2} + k_2 \frac{\partial^2 \theta}{\partial x^2} = \gamma \frac{\partial^2 u}{\partial t^2} \tag{1a}$$

$$k_3 \frac{\partial^2 u}{\partial x^2} + k_4 \frac{\partial^2 \theta}{\partial x^2} = \mu \frac{\partial^2 \theta}{\partial t^2} \tag{1b}$$

and the free vibration solution has been found to be

$$u(x,t) = \sum_{i=1}^{2} (u_0 a_i + \theta_0 c_i)\, w_i(x,t) \tag{2a}$$

$$\theta(x,t) = \sum_{i=1}^{2} (u_0 b_i + \theta_0 d_i)\, w_i(x,t) \tag{2b}$$

where in Eqs. (1) and (2), k_1–k_4 are stiffnesses; γ is the mass and μ is the mass moment of inertia about the axis per unit length of the spring; u_0 and θ_0 are initial axial and rotational displacements; and a_i, b_i, c_i, and d_i are coefficients. All of these constants can be found in the previous paper.

The free vibration of the spring is characterized by the function

$$\omega_i(x,t) = \begin{cases} (-1)^m \left(\dfrac{t}{\omega_i} - 2m + 1\right) \\ \qquad \left(2m - 1 - \dfrac{x}{h}\right)\omega_i \le t \le \left(2m - 1 + \dfrac{x}{h}\right)\omega_i \\ (-1)^m \dfrac{x}{h} \\ \qquad \left(2m - 1 + \dfrac{x}{h}\right)\omega_i \le t \le \left(2m + 1 - \dfrac{x}{h}\right)\omega_i \end{cases} \tag{3}$$

$$m = 0, 1, \ldots$$

which generaly represents a trapezoidal wave with period $4\omega_i$, and degenerates to a triangular wave at the free end. Analysis shows that the wave function $w_1(x,t)$ characterizes the longitudinal vibration, while $w_2(x,t)$ characterizes the torsional vibration of the spring. The spring vibration is a combination of these two waves. Because of the difference in period, the resultant wave is complex and not periodic.

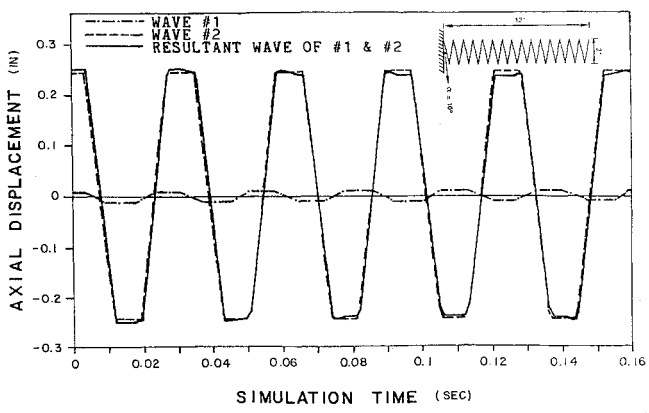

Fig. 1 Axial displacement at middle point due to wave 1, wave 2, and resultant wave of 1 and 2 for a helical angle of 10 deg and an initial axial displacement of 0.5 in.

To further explore the characteristics of the spring vibration, let us consider a helical spring 1 ft high, with a helix radius r of 1 in. The spring wire, of radius $R = \frac{1}{8}$ in., is assumed to be made of steel; Young's modulus is $E = 30$ Mpsi and Poisson's ratio is $\nu = 0.3$.

First consider the free vibration of the spring due to an initial displacement u_0 of 0.5 in. at the free end. The axial and rotational displacements for different helical angles are shown in Figs. 1–6.

Figure 1 shows the axial displacement, as a function of time t, at the middle point of the spring for a helical angle of 10 deg. It is the resultant of two trapezoidal waves. The periods of the longitudinal wave (marked as wave 1 in Fig. 1) and the rotational wave (marked as wave 2) are found to be 0.02731 and 0.03114 s, respectively. To study the interaction of these two waves, Fig. 7a gives amplitude ratios of the longitudinal wave vs the torsional wave, and Table 1 gives all of the detailed data. It is seen that in the case of small helical angles ($\alpha < 15$ deg), the amplitude ratio a_1/a_2 is less than 0.1, that is, the rotational wave prevails over the longitudinal wave. For example, in the case of $\alpha = 10$ deg, the longitudinal wave is so weak that the axial displacement is basically determined by the rotational wave. The rotational wave also dominates the axial velocity (Fig. 2) and the axial strain (Fig. 3). Therefore, the axial velocity wave and the axial strain wave are somewhat square and periodic.

For large helical angles, on the other hand, the influence of the longitudinal wave on the axial displacement becomes prominent. Table 1 shows that when the helical angle exceeds 75 deg, the amplitude ratio of a_1/a_2 is greater than 0.9 so that the longitudinal wave dominates the vibration and the spring behaves like a rod. As an example, Fig. 4 gives the axial displacement of the spring for a helical angle of 80 deg. It is seen that in such a case the period of the resultant wave is almost equal to the period of the longitudinal wave.

When the helical angle is in the range of 15–75 deg, the resultant wave shows a competition of the longitudinal and torsional waves. As a result, the resultant wave becomes irregular and not periodic. However, for the example considered, the periods of these two component waves differ not too much, as can be seen from Table 1 or Fig. 8, and beat thus

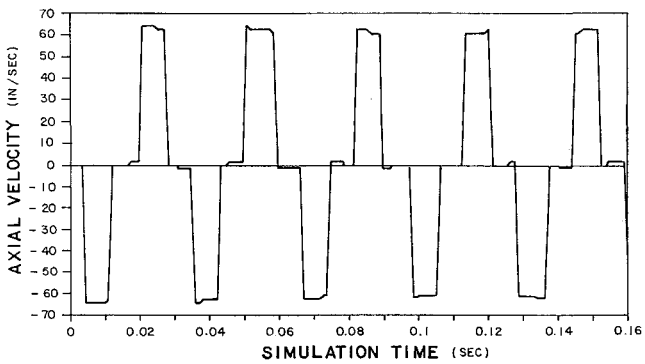

Fig. 2 Axial velocity at middle point due to resultant wave of 1 and 2 for a helical angle of 10 deg and an initial axial displacement of 0.5 in.

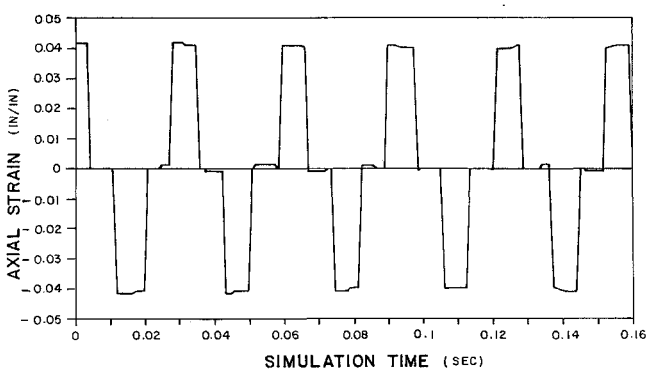

Fig. 3 Axial strain at middle point due to wave 1, wave 2, and resultant wave of 1 and 2 for a helical angle of 10 deg and an initial axial displacement of 0.5 in.

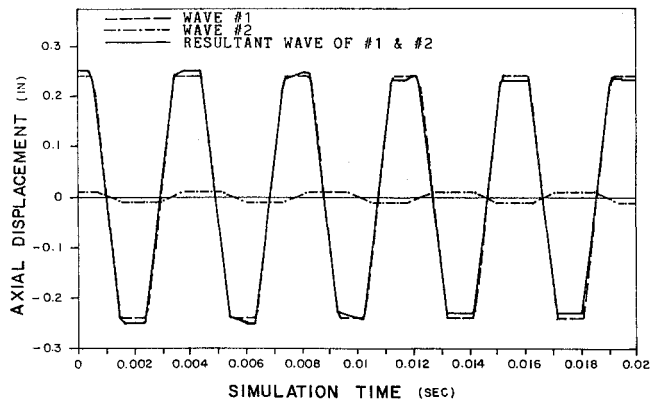

Fig. 4 Axial displacement at middle point due to wave 1, wave 2, and resultant wave of 1 and 2 for a helical angle of 80 deg and an initial axial displacement of 0.5 in.

Table 1 Periods and coefficients of waves for different helical angles

Helical angle, deg	Periods of waves, s			Coefficients of waves: Initial axial displacement u_0						Initial rotational displacement θ_0					
	$4\omega_1$	$4\omega_2$	ω_1/ω_2	a_1	a_2	a_1/a_2	b_1	b_2	$\lvert b_1/b_2 \rvert$	c_1	c_2	$\lvert c_1/c_2 \rvert$	d_1	d_2	d_1/d_2
5	0.05460	0.06226	0.87697	0.006	0.994	0.006	−0.068	0.088	0.773	−0.087	0.113	0.770	0.990	0.010	99.000
10	0.02731	0.03114	0.87701	0.024	0.976	0.025	−0.134	0.174	0.770	−0.169	0.220	0.768	0.961	0.039	24.641
15	0.01822	0.02078	0.87680	0.053	0.947	0.056	−0.197	0.257	0.767	−0.244	0.318	0.767	0.914	0.086	10.628
20	0.01368	0.01560	0.87692	0.093	0.907	0.103	−0.256	0.333	0.769	−0.309	0.402	0.769	0.852	0.148	5.757
25	0.01096	0.01250	0.87680	0.144	0.856	0.168	−0.309	0.403	0.767	−0.361	0.470	0.768	0.779	0.221	3.525
30	0.00915	0.01044	0.87644	0.204	0.796	0.256	−0.355	0.463	0.767	−0.400	0.521	0.768	0.697	0.303	2.300
35	0.00786	0.00897	0.87625	0.273	0.727	0.376	−0.393	0.512	0.768	−0.424	0.553	0.767	0.611	0.389	1.571
40	0.00691	0.00788	0.87690	0.349	0.651	0.536	−0.420	0.547	0.768	−0.435	0.566	0.769	0.524	0.476	1.101
45	0.00617	0.00704	0.87642	0.431	0.569	0.757	−0.437	0.569	0.768	−0.432	0.562	0.769	0.438	0.562	0.779
50	0.00559	0.00637	0.87755	0.517	0.483	1.070	−0.441	0.574	0.768	−0.417	0.542	0.769	0.355	0.645	0.550
55	0.00512	0.00584	0.87671	0.605	0.395	1.532	−0.431	0.561	0.768	−0.390	0.508	0.768	0.278	0.722	0.385
60	0.00475	0.00541	0.87800	0.692	0.308	2.247	−0.408	0.530	0.770	−0.354	0.460	0.770	0.208	0.792	0.263
65	0.00445	0.00507	0.87771	0.775	0.225	3.444	−0.369	0.479	0.770	−0.309	0.401	0.771	0.147	0.853	0.172
70	0.00421	0.00480	0.87708	0.849	0.151	5.623	−0.316	0.410	0.770	−0.256	0.333	0.769	0.095	0.905	0.105
75	0.00395	0.00449	0.87973	0.912	0.088	10.364	−0.250	0.325	0.769	−0.198	0.256	0.773	0.054	0.946	0.057
80	0.00391	0.00445	0.87865	0.960	0.040	24.000	−0.174	0.225	0.773	−0.134	0.174	0.770	0.024	0.976	0.025
85	0.00383	0.00436	0.87844	0.990	0.010	99.000	−0.089	0.115	0.774	−0.068	0.088	0.773	0.006	0.994	0.006

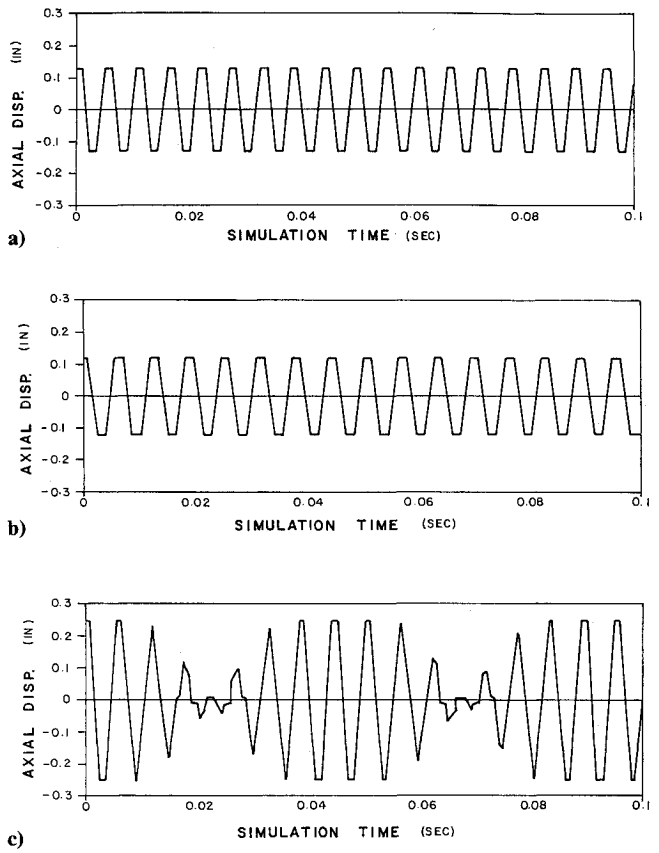

Fig. 5 Axial displacement at middle point due to a) wave 1, b) wave 2, and c) resultant wave of 1 and 2 for a helical angle of 50 deg and an initial axial displacement of 0.5 in.

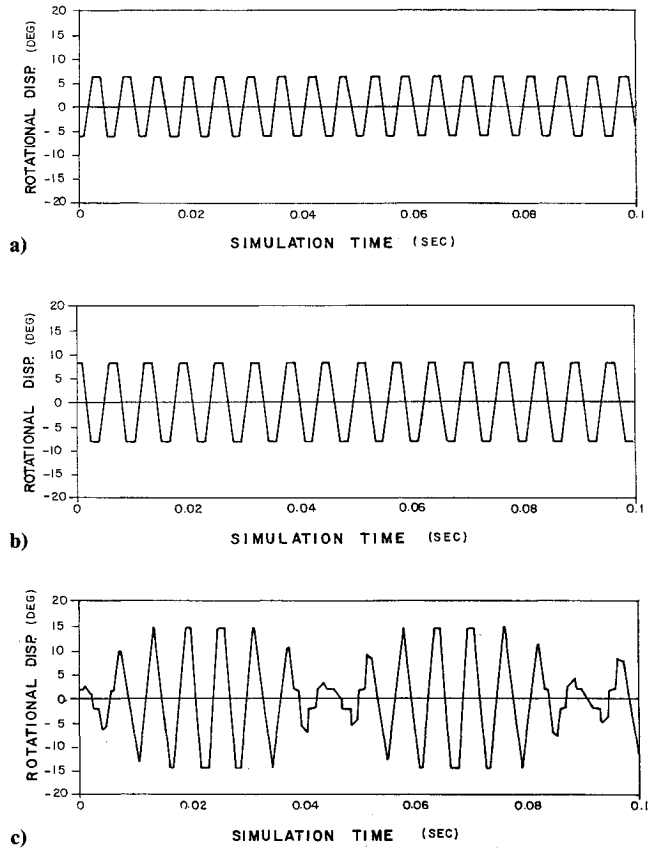

Fig. 6 Rotational displacement at middle point due to a) wave 1, b) wave 2, and c) resultant wave of 1 and 2 for a helical angle of 10 deg and an initial axial displacement of 0.5 in.

occurs. Figure 5 shows the phenomenon of beat for a helical angle of 50 deg. The beat period can be found as

$$T = 4\omega_1\omega_2/(\omega_2 - \omega_1) \tag{4}$$

Although the helical angle has a great influence upon the shape of the axial displacement wave, the shape of the rotational displacement wave turns out to be insensitive to the variation of the helical angle. In fact, it can be seen from Table 1 or Fig. 7a that the amplitude ratio b_1/b_2 varies within the range of 0.767–0.774 for any possible values of the helical angle. Thus, the rotational displacement always shows the interaction of the longitudinal and rotational waves, and consequently varies irregularly. Figure 6 gives the rotational displacement for a helical angle of 10 deg. The shapes of the rotational displacement for helical angles 50 and 80 deg look similar.

Now let us consider the free vibration of the spring caused by an initial rotational displacement θ_0 of 30 deg at the free end. The axial and rotational displacements at the middle point of the spring with a helical angle of 10 deg are shown in Figs. 9 and 10. To show the helical angle effect, the amplitude ratios c_1/c_2 and d_1/d_2 of the longitudinal wave vs the rotational wave are given in Table 1 and shown in Fig. 7b. It is

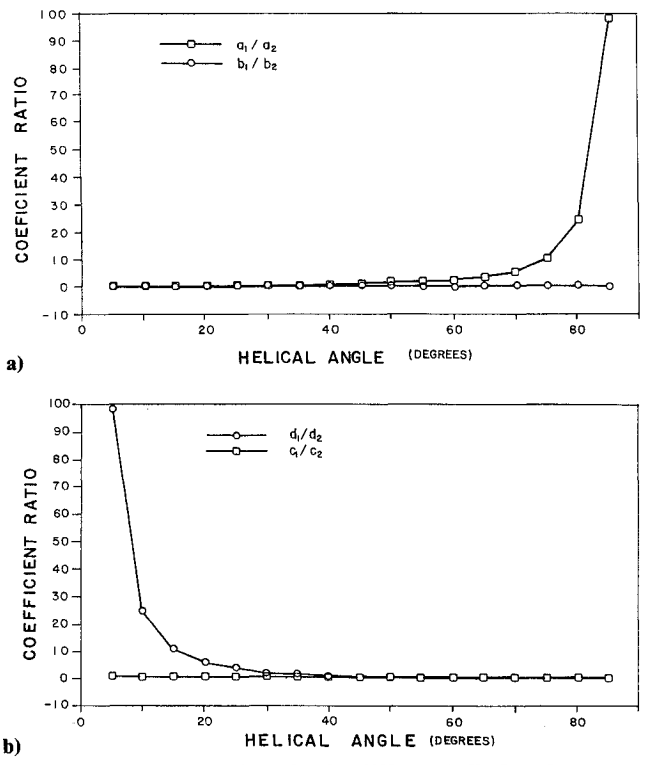

Fig. 7 Amplitude ratios for different helical angles.

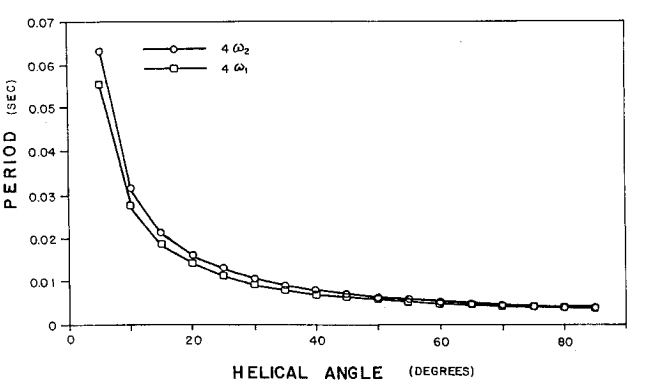

Fig. 8 Periods of waves 1 and 2 for different helical angles.

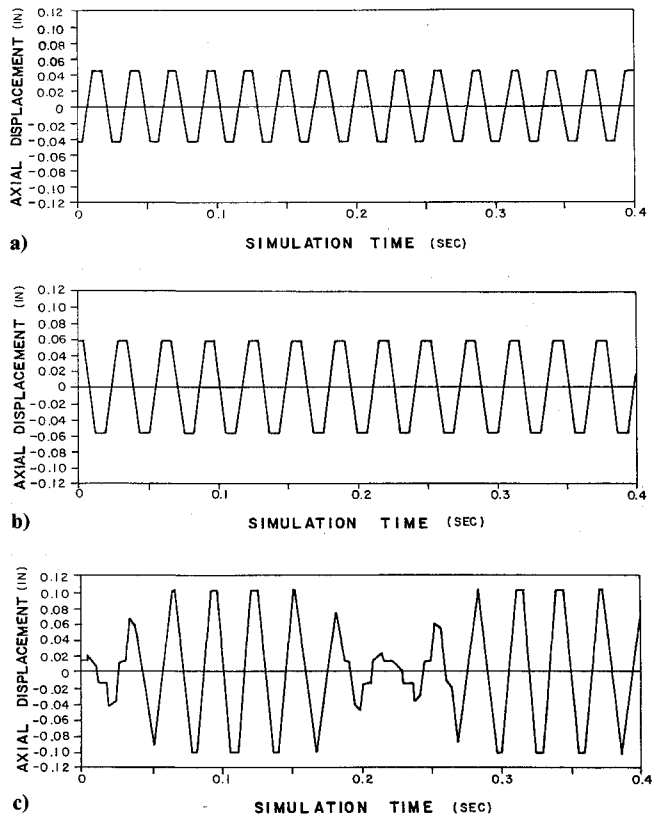

Fig. 9 Axial displacement at middle point due to a) wave 1, b) wave 2, and c) resultant wave of 1 and 2 for a helical angle of 10 deg and an initial rotational displacement of 30 deg.

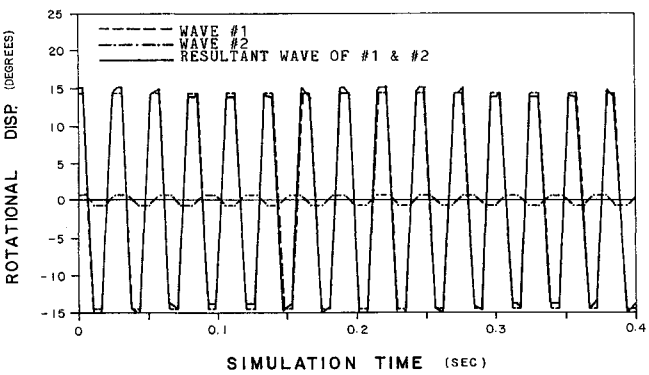

Fig. 10 Rotational displacement at middle point due to wave 1, wave 2, and resultant wave of 1 and 2 for a helical angle of 10 deg and an initial rotational displacement of 30 deg.

interesting to point out that contrary to the vibration caused by an initial axial displacement, the shape of the axial displacement wave in the present case is insensitive to the helical angle, while the shape of the rotational displacement wave is sensitive. Again, when the helical angle is less than 15 deg or greater than 75 deg, only one wave dominates. Otherwise, two waves compete and make the resultant wave complex and not periodic.

The periods of the component longitudinal and rotational waves are affected by the helical angle α, the ratio of the wire radius vs helix radius R/r, and the material properties. Table 1 shows that both these periods decrease with the increase of the helical angle, but the ratio of ω_1/ω_2 varies insignificantly, changing only from 0.876 to 0.880. Table 2 gives the period ratio for various R/r ratios for a helical angle of 5 deg. It is seen that this period ratio is nearly a constant of 0.877. Now considering the same spring with a helical angle of 5 deg, but changing the material to cast iron (E = 24 Mpsi and ν = 0.290)

Table 2 Periods of waves for different R/r ratio

R/r	R, in.	r, in.	$4\omega_1$, s	$4\omega_2$, s	ω_1/ω_2
1/32	0.0625	2.0	0.21841	0.24903	0.87704
1/16	0.1250	2.0	0.10920	0.12451	0.87704
1/8	0.1250	1.0	0.05460	0.06226	0.87697
3/16	0.1875	1.0	0.03640	0.04151	0.87690
1/4	0.2500	1.0	0.02730	0.03113	0.87697
5/16	0.3125	1.0	0.02184	0.02491	0.87676
3/8	0.3750	1.0	0.01820	0.02076	0.87669
7/16	0.4375	1.0	0.01560	0.01779	0.87690
1/2	0.2500	0.5	0.01365	0.01557	0.87669

and then to yellow brass (E = 15 Mpsi and ν = 0.339), we find that the period ratio equals 0.88048 and 0.86415, respectively. From all of these data it appears that, for the spring configuration chosen, the period ratio of the spring is nearly a constant, and the periods of two component waves differ only a little. Thus, the beat will usually occur in the free vibrations of the spring.

Finally, an interesting phenomenon is worth pointing out. It can be seen that when the free vibration is caused by an initial axial displacement, the axial displacement cannot exceed, at any time, the initial value, which is obvious from the viewpoint of energy conservation. However, the rotational displacement can be much larger than its initial value, as also can be seen from the figures. The explanation is that, for the coupled system, the energy is stored in two forms: the extensional-compressive energy and the torsional energy. Because of the beat phenomenon, the amplitude of the resultant wave varies. Therefore, when the amplitude of the axial displacement reaches its minimum, a large part of the extensional-compressive energy is transferred to the torsional energy, and that makes the amplitude of the rotational displacement exceed its initial value. Similarly, we can see that if the free vibration is caused by an initial rotation, the axial displacement can be greater than its initial value, but the rotational displacement cannot.

Conclusions

Because of the coupled behavior, two waves propagate through the spring. As is well known, the sum of two harmonic motions of different frequencies is not harmonic. The free vibration of the helical springs is thus much more complex than we used to think it to be. However, the examples used in this research show that the period ratio of these two waves is nearly a constant and these two periods do not differ too much, notwithstanding the differences in helical angles, R/r ratios, and material properties. Consequently, the beat phenomenon often occurs in the free vibration of helical springs, which makes the vibration appear periodic.

References

[1]Michell, J. H., "The Small Deformation of Curves and Surfaces with Application to the Vibrations of a Helix and a Circular Ring," *Mess. Math,* Vol. 19, 1890, pp. 68–82.

[2]Love, A. E. H., "The Propagation of Waves of Elastic Displacement Along a Helical Wire," *Transactions of the Cambridge Philosophical Society,* Vol. 18, 1899, pp. 364–374.

[3]Yoshimura, Y., and Murata, Y., "On the Elastic Waves Propagated Along Coil Springs," *Rep. Inst. Sci. and Tech. Tokyo University,* Vol. 6, No. 1, 1952, pp. 27–35.

[4]Wittrick, W. H., "On Elastic Wave Propagation in Helical Springs," *International Journal of Mechanical Science,* Vol. 8, No. 25, 1966, pp. 25–47.

[5]Mottershead, J. E., "Finite Elements for Dynamical Analysis of Helical Rods," *International Journal of Mechanical Science,* Vol. 22, No. 5, 1980, pp. 267–283.

[6]Pearson, D., and Wittrick, W. H., "An Exact Solution for the Vibration of Helical Springs Using a Bernoulli-Euler Model," *International Journal of Mechanical Science,* Vol. 28, No. 2, 1986, pp. 83–96.

[7]Pearson, D., "Dynamic Behavior of Helical Springs," *Shock and Vibration Digest,* Vol. 20, No. 7, 1988, pp. 3-9.
[8]Dick, J., "Shock-Waves in Helical Springs," *The Engineer,* Vol. 204, Aug. 9, 1957, pp. 193-195.
[9]Gross, S. C., "Coil Spring Performance," *Automobile Engineering,* 1959.
[10]Curran, J. P. S., "Further Considerations in Injector Design for High Specific Output Diesel Engines," *I. Mech. E. Symp,* Critical Factors in the Application of Diesel Engines, Southhampton Univ., 1970.
[11]Phillips, J. W., and Costello, G. A., "Large Deflections of Impacted Helical Springs," *Journal of the Acoustical Society of America,* Vol. 51, No. 3, Pt. 2, 1972, pp. 967-973.
[12]Costello, G. A., "Radial Expansion of Impacted Helical Springs," *Journal of Applied Mechanics, Transactions of the ASME,* Vol. 42, Dec. 1975, pp. 789-792.
[13]Sinha, S. K., and Costello, G. A., "The Numerical Solution of the Dynamic Response of Helical Springs," *International Journal for Numerical Methods in Engineering,* Vol. 12, 1978, pp. 949-961.
[14]Jiang, W., Jones, W. K., Wang, T. L., and Wu, K. H., "Free Vibration of Helical Springs," *Journal of Applied Mechanics, Transactions of ASME,* Vol. 58, No. 1, 1991, pp. 222-228.

Collapse Characteristics of Cylindrical Composite Panels Under Axial Loads

S. A. Schimmels* and A. N. Palazotto†
Air Force Institute of Technology,
Wright-Patterson Air Force Base, Ohio 45433

Introduction

LAMINATED composites are well suited for membrane applications, but structurally optimizing an elastic shell makes it susceptible to buckling or collapse. Shells such as stiffened fuselage panels contain many discontinuities, such as square cutouts, which cause local stress and displacement gradients that influence structural performance. The phenomenon of buckling of flat composite panels or plates is well documented and not discussed herein. The instability of curved composite panels is attracting a smaller amount of documented research,[1,2] and only recently are there articles including work on composite shells requiring nonlinear analysis due primarily to the inclusion of geometric discontinuities (such as cutouts) within their structure.[3] In this Note, the static response of a laminated graphite/epoxy cylindrical shell subjected to an axially distributed load considering cutout positioning is investigated. A 36-degree-of-freedom (DOF) two-dimensional curved, rectangular finite element, including through-the-thickness transverse shear, is incorporated in this study. A modified Newton-Raphson (MNR) iterative technique traces equilibrium through to the collapse load and comparisons are made to experimentation.

Numerical Modeling

Comparable theories incorporating higher-order transverse shear effects for laminated shells were presented by Reddy and Liu[4] and Dennis and Palazotto.[5] The code, with a 36-DOF element mentioned previously and referred to as SHELL, is used herein. SHELL's theory is thoroughly discussed in Ref. 5. An important aspect of the present study is to determine the effect of transverse shear strain (while considering large displacements and rotations) on a cylindrical shell. Transverse shear strain β_s is defined as

$$\beta_s = |\Psi_s| - |w_{,s}| \tag{1}$$

where Ψ_s is the rotation due to the bending, β_s the rotation due to transverse shear, and $w_{,s}$ the slope of the elastic curve. Since Ψ_s and $w_{,s}$ are degrees of freedom calculated by SHELL, the difference of their magnitudes must equal the change in the slope of the elastic curve in the presence of transverse shear strain.

A convergence study was conducted using the 36-DOF element. This study led to the refined mesh shown for the two basic panels (see Fig. 1). In considering imperfections (cutouts) of the 4 in. × 4 in. size, circumferential eccentricity of 1 in. was included in the study, as shown in Fig. 2. The mesh size used in this study resulted in a general set of active DOF equal to approximately 2750 for the 8-in. panel and 3300 for the 12-in. panel.

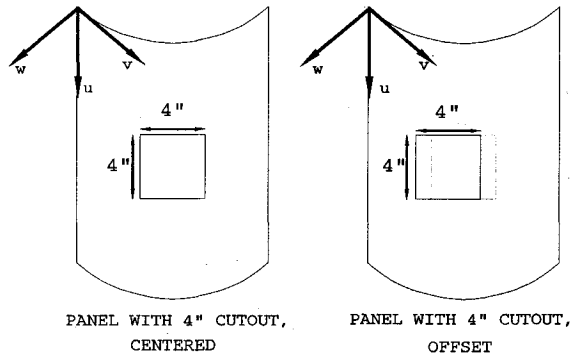

Fig. 1 Location of cutouts studied.

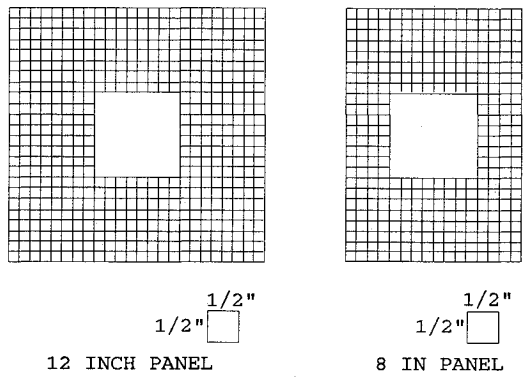

Fig. 2 Refined meshes for 8×12 in. and 12×12 in.

Results and Discussion

References 6 and 7 discuss the experimental test setup and the axial compression procedure in detail. Graphite/epoxy panels (Hercules AS4-3501-6) were studied with the following properties:

$$E_1 = 20.461 \times 10^6 \text{ psi}$$

$$G_{12} = 0.883 \times 10^6 \text{ psi}$$

$$E_2 = E_3 = 1.468 \times 10^6 \text{ psi}$$

$$G_{13} = G_{23} = 0.441 \times 10^6 \text{ psi}$$

$$\nu_{12} = 0.28$$

with a ply-lay up of $[0, \mp 45, 90]_s$.

Received Oct. 15, 1990; revision received July 23, 1991; accepted for publication July 31, 1991. This paper is declared a work of the U.S. Government and is not subject to copyright protection in the United States.

*Ph.D. Candidate, Aeronautics and Astronautics Department.
†Professor, Aeronautics and Astronautics Department. Associate Fellow AIAA.